Proc of the 2025 IEEE International
Conference on Real-time Computing and Robotics
June 1 - 6, 2025, Toyama, Japan

2025 IEEE International Conference on Real-time Computing and Robotics (RCAR) | 979-8-3315-0205-8/25/$31.00 ©2025 IEEE | DOI: 10.1109/RCAR65431.2025.11139413

FMCW Millimeter-Wave Radar-Based Remote Monitoring of Vital Signs in Multiple Subjects

Dezhi Yu, Hao Zhou, Xiaohui Li, Wenzhou Wang, Jinfeng Huang, Xin'an Wang,
Guanglin Li and Lin Wang*, Member, IEEE

***Abstract*— Traditional methods for measuring vital signs often require hospital visits and direct skin contact, making them costly and operationally inconvenient. However, advancements in millimeter-wave radar technology have enabled non-contact monitoring of vital signs, particularly in close-range, single-subject scenarios. Despite this progress, challenges persist in simultaneously monitoring multiple subjects over extended distances. This paper investigates the feasibility of long-range, multi-subject vital sign monitoring using frequency-modulated continuous-wave (FMCW) radar technology. In this study, we first determined the subject distances and angles through radar measurements. To enhance the accuracy of breathing rate (BR) and heart rate (HR) estimations, we coherently accumulated phase information from multiple subjects. Noise interference was mitigated using first-order difference and moving average filtering techniques. Adaptive filters were also developed to effectively separate the breathing and cardiac signals. Finally, spectral estimation algorithms were employed to accurately calculate BR and HR. Experimental results demonstrated that when subjects were positioned within 1.5 m, the root mean square error (RMSE) for both BR and HR remained below 2. At a distance of 3.0 m, the RMSE for BR and HR increased but remained below 4. By varying the subject-radar distances and angular configurations, the proposed method was validated for its effectiveness and precision in long-range, multi-subject monitoring scenarios.**

I. INTRODUCTION

Monitoring vital signs, particularly breathing rate and heart rate, is of considerable importance in both the medical field and daily life. The breathing rate and heart rate carries valuable health insights that can guide effective treatments and preventive measures for both doctors and patients[1]. Currently, vital sign monitoring is primarily categorized into contact-based[2] and non-contact-based methods[3]. The contact method, mainly in the form of electrocardiograms (ECG)[4], offers the advantage of highly accurate and reliable results. However, it can be inconvenient for patients, as they often need to visit a medical facility for testing. Moreover, contact-based methods are not suitable for patients with severe burns or skin conditions. Non-contact methods, such as cameras and radar, offer distinct benefits. Cameras, for instance, do not require physical contact with the patient's body, helping to avoid secondary injuries. However, the use of cameras raises concerns related to personal privacy.

Widely used radar technologies to monitor breathing rate and heart rate include Ultra-Wideband Radar (UWB)[5], Continuous Wave Radar (CW)[6], and Frequency Modulated Continuous Wave Millimeter-Wave Radar (FMCW mm-radar)[7]. UWB radar offers significant advantages due to its strong penetration capabilities, allowing for effective monitoring in complex environments. However, UWB is sensitive to interference from other signals, which can compromise measurement accuracy. In contrast, CW radar features a simple hardware structure and high monitoring precision, but its range is limited, making it suitable only for close-range monitoring. FMCW millimeter-wave radar, on the other hand, is less prone to interference and is capable of performing long-range monitoring[8]. The shorter wavelength of millimeter waves enhances sensitivity to dynamic body movements, enabling the detection of subtle surface changes, thereby improving the accuracy of breathing rate and heart rate monitoring[9].

Millimeter-wave radar has become widely adopted in recent studies for monitoring human breathing rate and heart rate. However, to ensure measurement accuracy, it is typically necessary for the subject to be positioned within a relatively short range from the radar[10], usually within 1.5 m. The subject's posture is also crucial, as they must be positioned directly in front of the radar to ensure that the radar signal is accurately focused on the chest, minimizing noise interference and enhancing monitoring precision for both breathing rate and heart rate. When extracting breathing rate and heart rate information from the phase of received signals, it is common practice to sample data from a single range bin[11]. However, the human body's reflected signal often spans multiple range bins, which can lead to lower accuracy when phase estimation for breathing rate and heart rate is based solely on a single range bin. In vital sign monitoring, the same algorithm is typically used to extract both breathing rate and heart rate signals. However, certain algorithms may perform better for breathing rate signal

*This work was supported in part by Shenzhen Sustainable Development Sci-Tech project (Grant KCXFZ20230731093501003), in part by Shenzhen Science and Technology Program (Grant XMHT20230115002) , and in part by Shenzhen Strategic Emerging Industry Support Plans (Grant KQTD20210811090217009).(*corresponding author: Lin Wang. e-mail: lin.wang1@siat.ac.cn)

Dezhi Yu and Xiaohui Li are with Shenzhen Institutes of Advanced Technology, Chinese Academy of Sciences, China, also with University of Chinese Academy of Sciences, China, and also with The Shenzhen Lower Limb Rehabilitation Intelligent Aids Engineering Research Center, China. (email: dz.yu@siat.ac.cn;xh.li1@siat.ac.cn).

Jinfeng Huang and Xin'an Wang are with the School of Software & Microelectronics, Peking University, Beijing 102600, China. (email: jfhuang@stu.pku.edu.cn;anxinwang@pku.edu.cn).

Hao Zhou, Wenzhuo Wang, Guanglin Li and Lin Wang are with Shenzhen Institutes of Advanced Technology, Chinese Academy of Sciences, China, and also with The Shenzhen Lower Limb Rehabilitation Intelligent Aids Engineering Research Center, China.(e-mail: h.zhou@siat.ac.cn; wz.wang2@siat.ac.cn;gl.li@siat.ac.cn; lin.wang1@siat.ac.cn).

extraction while being less accurate for heart rate signals[12]. Additionally, interference from breathing harmonics, subtle body movements, and environmental clutter can further complicate the extraction of accurate heart rate data[13].

This paper presents a method for long-range monitoring (up to 3.0 m) of multiple subjects in an indoor environment. Initially, we determine the distance and angle of the subject relative to the radar and identify the range bins occupied by the subject. Coherent accumulation is then performed to enhance signal quality. Subsequently, we extract vital sign signals by unwrapping the phase using the arctangent and applying a first-order difference to capture the time-varying phase. A filtering technique is employed to separate the breathing rate and heart rate signals. Finally, the Multiple Signal Classification (MUSIC) algorithm[14] is used for spectral estimation of the breathing rate signal to extract the breathing rate , while 2D-FFT (2D Fast Fourier Transform) is applied to estimate the heart rate from the heartbeat signal. The main contributions of this paper are as follows:

- By selecting the two range bins with the highest backscattering energy for coherent accumulation, phase information is extracted. Different spectral estimation algorithms are then used to analyze the breathing and heartbeat signals, thereby extracting the breathing rate and heart rate.
- Extensive experiments demonstrate that the proposed method can simultaneously monitor the breathing rate and heart rate of multiple subjects, providing high-precision estimation results under different subject offset angles and distance scenarios relative to the radar.

The remainder of this paper is structured as follows: Section II details the implementation of the breathing rate and heart rate monitoring algorithm. Section III presented and discussed the experimental results. Finally, Section IV provides the conclusions of the paper.

II. METHOD

In this section, we provide a detailed description of the process for detecting human breathing and heartbeat, which consists of three steps: target detection, target phase extraction and processing, and extraction and analysis of breathing and heartbeat signals.

A. Target Detection

Before extracting the target phase, it is necessary to first detect the human target and determine its distance and angle relative to the radar. FMCW radar can obtain the target's distance information. The intermediate frequency (IF) signal is digitized and organized by the analog-to-digital converter (ADC), generating an N×M two-dimensional matrix, where N represents the number of sampling points per chirp, referred to as the fast time, and M represents the number of sampled frames, referred to as the slow time[15]. For the fast-time sampling data of M frames, the range-FFT[16] method is used for processing to obtain M spectrum plots. Since there is a one-to-one correspondence between frequency and target distance, the frequency information in the spectrum can be converted to the target distance, generating the corresponding distance spectrum as shown in Fig.1.

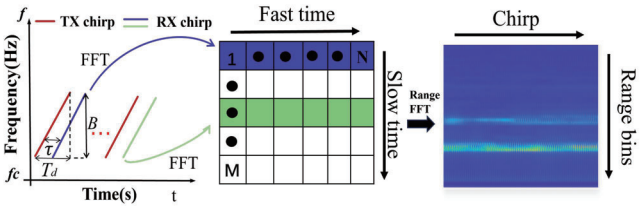

Fig. 1: FMCW radar signa.l

B. Phase Extraction and Processing

After completing the detection of the human position, it is necessary to extract and process the phase information of the range bin where the human body is located. After performing Range-FFT, the resulting data is in the complex form where a is the real part, b is the imaginary part, and i is the imaginary unit. We use the arctangent method[17] to extract the phase information and calculate the phase angle θ using the arctangent.

$$\theta = \arctan\left(\frac{b}{a}\right) \tag{1}$$

The phase angle θ is determined by the ratio of the imaginary part b to the real part a of a complex number. The arctangent provides the angle in the first and fourth quadrants. However, to correctly determine the phase angle across all quadrants, adjustments are made based on the signs of a and b. Specifically, when a is negative, the angle is adjusted by subtracting from π or adding to -π, depending on the sign of b. When b is negative, the negative sign is factored into the arctangent calculation or applied to the result, ensuring the phase angle is correctly oriented in the respectivequadrant.

If $a > 0$ and $b > 0$, then the phase angle θ is given by (1).
If $a < 0$ and $b > 0$, then the phase angle θ is given by

$$\theta = \pi - \arctan\left(\frac{|b|}{|a|}\right) \tag{2}$$

If $a < 0$ and $b < 0$, then the phase angle θ is given by

$$\theta = -\pi - \arctan\left(\frac{|b|}{|a|}\right) \tag{3}$$

If $a > 0$ and $b < 0$, then the phase angle θ is given by

$$\theta = -\arctan\left(\frac{|b|}{a}\right) \tag{4}$$

Since the subject may span multiple range bins, we accumulate the phases of the two range bins with the highest echo strength. After phase extraction, to obtain accurate true phase values, phase unwrapping is required to address phase jumps caused by physiological factors such as breathing rate[18]. Phase values are inherently periodic within the range of $[-\pi, \pi]$, and the directly measured phase values may not accurately reflect the true phase distribution of the subject

due to this periodic wrapping. Phase unwrapping techniques remove these phase folds, allowing for the recovery of continuous phase variations and thus providing the true phase information over a broader range. This process is a critical step for accurately analyzing subject motion characteristics and extracting valuable physiological signals[19]. The main idea is as follows: the phase of the subsequent data point is sequentially subtracted from the phase of the previous data point. If the difference exceeds π, the subsequent phase value should be adjusted by subtracting 2π. If the difference is less than $-\pi$, the subsequent phase value should be adjusted by adding 2π. If the difference lies between $-\pi$ and π, no adjustment is necessary.

Millimeter-wave radar monitors breathing rate and heart rate based on the phase changes in the FMCW signals at specific range bins, which are caused by the chest's micro-movements resulting from breathing and heartbeat. The phase of the transmitted signal is given by:

$$\varphi_T(t) = 2\pi \left(f_c t + \frac{1}{2} S t^2 - S_m T_{RRI} t \right) \quad - \theta_0(m) + \varphi(t) \tag{5}$$

The phase of the received signal:

$$\varphi_R(t) = 2\pi \left(f_c(t-\tau) + \frac{1}{2} S(t-\tau)^2 - S_m T_{RRI}(t-\tau) \right) - \theta_0(m) + \varphi(t-\tau) \tag{6}$$

The phase of the intermediate frequency (IF) signal, which is obtained by mixing the transmitted and received signals followed by low-pass filtering:

$$\begin{aligned} \varphi_{IF}(t) &= \varphi_T(t) - \varphi_R(t) \\ &= 2\pi \left[f_c \tau - \frac{1}{2} S \tau^2 + S\tau(t - m T_{RRI}) \right] + \Delta\varphi_t \end{aligned} \tag{7}$$

The distance between the subject and the radar is $R(t) = R_0 + x(t)$ where $x(t)$ represents the relative displacement between the subject and the radar caused by the subject's chest micro-motions. The time delay between the received and transmitted signals is given by $\tau = \frac{2R(t)}{c}$ where c is the speed of light. Substituting this into equation (4), we get:

$$\begin{aligned} \varphi_{IF}(t) = 2\pi \Bigg[& f_c \frac{2(R_0 + x(t))}{c} - \frac{1}{2} S \left(\frac{2R_0 + x(t)}{c} \right)^2 \\ & + S \left(\frac{2R_0 + x(t)}{c} \right) (t - m T_{RRI}) \Bigg] + \Delta\varphi_t \end{aligned} \tag{8}$$

By neglecting the second term and phase noise and phase noise$\Delta\varphi_t$, let $t_m = t + mT_{RRT}$,then $t = t_m + T_{RRT}$,we get:

$$\begin{aligned} \varphi_{IF}(t_m) = & 2\pi S \left(\frac{2(R_0 + (t_m + m T_{RRI}))}{c} \right) t_m \\ & + \frac{4\pi \left(R_0 + x(t_m + m T_{RRI}) \right)}{\lambda_c} \end{aligned} \tag{9}$$

Here, t represents an arbitrary moment within any chirp period, referred to as fast time, while t_m represents an arbitrary moment within the m-th chirp period, referred to as slow time. From equation (6), it is known that the initial distance R_0 between the subject and the radar, as well as the initial relative displacement $x(t_m + mT_{RRI})$ between the subject and the radar, modulate the phase of the intermediate frequency (IF) signal simultaneously:

$$\begin{aligned} \varphi_{IF} &= \frac{4\pi(R_0 + x(t_m + m T_{RRI}))}{\lambda_c} \\ &= \frac{4\pi x(t_m + m T_{RRI})}{\lambda_c} + \frac{4\pi R_0}{\lambda_c} \end{aligned} \tag{10}$$

In respiratory signal modulation, the phase components involve both time-varying phase $\frac{4\pi x(t_m + mT_{RRI})}{\lambda_c}$ and a constant phase offset $\frac{4\pi R_0}{\lambda_c}$ caused by the initial distance between the subject and the radar. To extract the time-varying phase, it is necessary to remove the constant phase offset. A common approach to achieve this is through first-order difference operation. Specifically, by computing the phase difference between the intermediate frequency (IF) signal of the current frame and the previous frame, the constant phase offset can be effectively eliminated. Since the phase of all frames contains the same constant phase offset, the phase difference between consecutive frames helps to cancel out this offset, thereby enhancing the heartbeat signal in the process. After these steps, the time-varying signals of breathing rate and heartbeat are obtained. However, due to the interference from random body movements and environmental noise, a sliding average filter is applied to the first-order differenced signal to effectively suppress noise components and achieve signal smoothing.

C. Extraction and Analysis of BR and HR Signals

Finally, an IIR elliptical bandpass filter with a frequency range of 0.1–0.5 Hz was applied to filter the signal, preserving the respiratory signal. An IIR elliptical bandpass filter with a frequency range of 0.8–2 Hz was then used to filter the signal, preserving the heartbeat signal. Subsequently, the MUSIC was applied for spectral estimation of the respiratory signal, while the 2D-FFT was used for spectral estimation of the heartbeat signal. By identifying the peaks in the frequency spectrum, the corresponding frequencies of the breathing and heartbeat signals were determined.

III. Experimental Results and Discussion

A. Experimental Parameters

In this paper, the IWR6843ISK millimeter-wave radar sensor from Texas Instruments (TI) was used [20]. This sensor is a single-chip FMCW radar system that integrates modules such as a phase-locked loop, transmitter, receiver, baseband circuits, and ADC, with an operating frequency range of 60 GHz to 64 GHz. The IWR6843ISK radar is configured with a two-transmit and four-receive antenna array and operates in time-division multiplexing (TDM) mode, alternately driving antennas TX1 and TX2 to transmit frequency-modulated pulses, thus synthesizing eight virtual

antenna arrays. The specific operational parameters of the FMCW radar are detailed in Table I.

TABLE I: CHIRP PARAMETERS USED IN THIS WORK

Start Frequency,f_c (GHz)	60
Frequency Slope, S (MHz/μs)	60
Idle Time (μs)	7
TX Start Time (μs)	1
ADC Start Time (μs)	6
ADC Samples	128
ADC Sample Rate (MHz)	3
Ramp End Time (μs)	60
Number of chirps Per Subframe	1
Frame Periodicity (ms)	50

We combined the IWR6843ISK radar with the DCA1000EVM data acquisition board [21], which generates AD sampled binary data files through the DCA1000EVM. These binary data files are then analyzed using algorithms to obtain breathing rate and heart rate. The experimental setup is shown in Figs.2 (a) and (b). We investigated the impact of the subject's distance from the radar and the subject's relative angle to the radar on breathing and heart rate monitoring. As shown in the schematic diagram of Fig.2 (a). We set different distances of 0.5 m, 1.0 m, 1.5 m, 2.0 m, and 3.0 m, while the angles were plotted in an arc starting from the midline. Solid lines were drawn at 15° intervals on both sides to represent angles of -60°, -45°, -30°, -15°, 0°, 15°, 30°, 45°, and 60°. First, we determined the initial distance of the subject, and under the condition of maintaining this distance, we varied the subject's angle. A total of 48 experiments were conducted, covering various distance and angle configurations. Four volunteers participated in the experiment. As shown in Fig.3, we used the ElasTech breathing belt and the Polar heart rate belt to collect breathing signals and heartbeat signals. Each data collection lasted 30 seconds, and the average breathing rate and heart rate during this period were compared with those obtained from the breathing and heart rate belts.

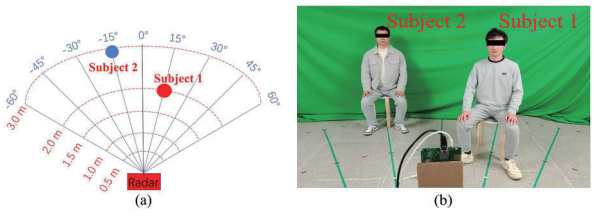

Fig. 2: Experimental scene.

To evaluate the accuracy of our algorithm in vital sign detection, we used estimation accuracy metrics from[22], including Mean Absolute Error (MAE) and Root Mean Squared Error (RMSE). MAE and RMSE are commonly used metrics for evaluating the predictive performance of regression models, with lower values indicating smaller prediction errors. The two differ in how they handle errors: RMSE is more sensitive to larger errors because its calculation involves squaring the error, which amplifies the impact of deviations. As a result, it is more suitable for situations where large errors are of particular concern. In contrast, MAE assigns equal weight to all errors, avoiding the disproportionate influence of extreme values, and is more appropriate when errors are distributed evenly.

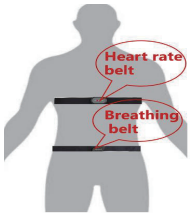

Fig. 3: Schematic diagram of the breathing belt and heart rate belt.

B. Results

Examples results of the breathing rate and heart rate for multiple subjects are shown in Table II and Table III.

TABLE II: COMPARISON OF RADAR-MONITORED BR WITH GROUND TRUTH(BPM)

Group	Subject	Distance	Angle	BR(RADAR)	Ground Truth
Group 1	Subject 1	0.5 m	-60°	22	20
	Subject 2	1.0 m	-30°	17	16
Group 2	Subject 3	1.0 m	30°	18	18
	Subject 4	1.5 m	-15°	24	24
Group 3	Subject 3	2.0 m	-45°	15	17
	Subject 4	3.0 m	45°	19	21

TABLE III: COMPARISON OF RADAR-MONITORED HR WITH GROUND TRUTH(BPM)

Group	Subject	Distance	Angle	BR(RADAR)	Ground Truth
Group 1	Subject 1	0.5 m	-60°	72	73
	Subject 2	1.0 m	-30°	78	80
Group 2	Subject 3	1.0 m	30°	82	75
	Subject 4	1.5 m	-15°	78	80
Group 3	Subject 3	2.0 m	-45°	68	71
	Subject 4	3.0 m	45°	70	71

As for the detection results of multi-subject breathing rate, as shown in Figs. 4 (a) and (b) , the accuracy is nearly 100% at distances of 0.5 m, 1.0 m, and 1.5 m. However, in Fig.4 (c) , at distances of 2.0 m and 3.0 m, the accuracy drops

to 87.5% and 75%, respectively. In addition, Fig.5 illustrates the model's estimation errors at these distances, showing that the MAE and RMSE values are both less than 3, indicating that the algorithm exhibits high accuracy and low prediction errors at close distances.

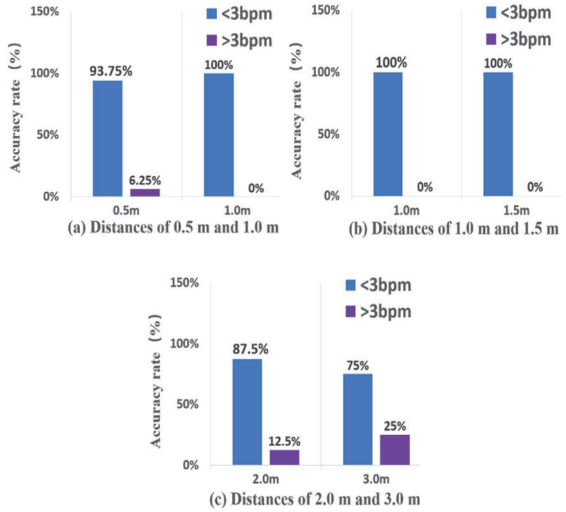

Fig. 4: Accuracy on multi-subject BR estimation.

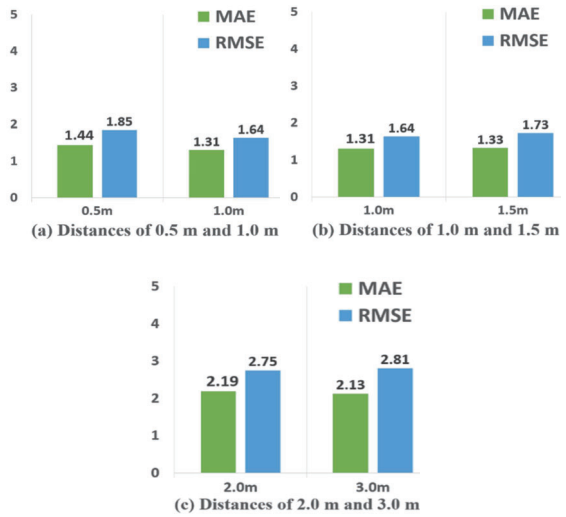

Fig. 5: Errors for multi-subject BR estimation.

Regarding the detection results of heart rate, as shown in Figs. 6 (a) and (b), the accuracies are 81.25%, 87.5%, and 87.5% at distances of 0.5 m, 1.0 m, and 1.5 m, respectively. In Fig.6 (c), at distances of 2.0 m and 3.0 m, the accuracies decrease to 75% and 68.75%, respectively. In Fig.7, further presents the MAE and RMSE values at different distances. In Figs. 7 (a) and (b), at the 1.5-meter range, both MAE and RMSE are less than 3, indicating that the model can accurately detect the heart rate at this distance. However, as shown in Fig.7 (c), at distances of 2.0 m and 3.0 m, the MAE values are 3.31 and 3.68, and the RMSE values are 3 and 3.61, respectively, indicating that as the subject distance increases, the errors also increase, though they remain within an acceptable range.

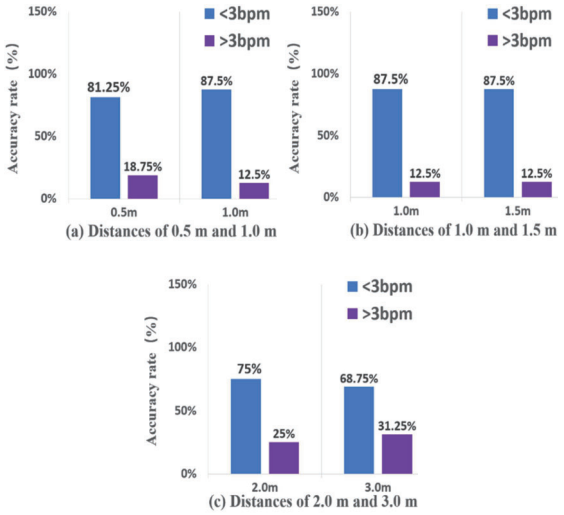

Fig. 6: Accuracy on multi-subject HR estimation.

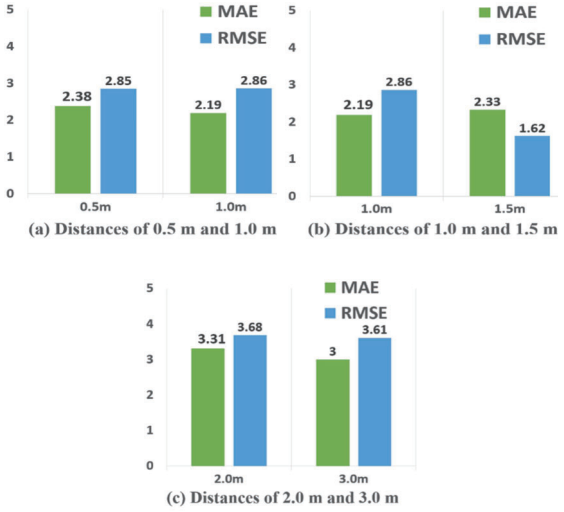

Fig. 7: Errors for multi-subject HR estimation.

C. Discussion and Comparison

The results of this study indicate that when the subject is within 1.5 m of the radar, the average error in both breathing rate and heart rate remains below 3 bpm. However, as the subject moves beyond 2.0 m, the errors in both parameters gradually increase, exceeding 3 bpm. Additionally, the study reveals that as the relative angle between the subject and the radar increases, the measurement error also tends to rise. Detection accuracy is notably higher when the subject's deviation angle is less than 45°. As shown in Table IV, a comparison with existing literature highlights a clear advantage in detection accuracy, especially in long-range monitoring scenarios.

In multi-subject close-range detection (e.g., at 0.5 meters), occlusion can occur when the angle between the subjects

is small, leading to a decrease in detection accuracy for the occluded subject. The limited sample size and number of participants in this study may affect the generalizability of the results to broader populations, which is a notable limitation. Given the time and resource constraints, future research could focus on improving the monitoring accuracy of subjects at larger radar angles, as well as detecting vital signs of subjects in different postures. Additionally, enhancing the accuracy of long-range multi-target detection could greatly expand the potential applications of this technology.

TABLE IV: COMPARISON TO OTHER WORKS

Ref.	Distance	BR(RMSE)	HR(RMSE)
2022,Z.Xu et al [22]	$< 2m$	> 3	> 3
2023,S.Ahmed et al [23]	$< 2m$	> 3	> 4
This study	$> 2m$	< 3	< 2 (1.5m),< 4 (3.0m)

IV. CONCLUSIONS

Improving the accuracy of FMCW millimeter-wave radar for monitoring the breathing rate and heart rate of multiple subjects at a long distance has been a key issue in radar-based vital sign monitoring. This paper details the various steps in radar data signal processing and the related parameter settings, proposing different methods for extracting respiratory and heartbeat signals, and comparing the results with those obtained from contact-based sensor devices (such as breathing belts and heart rate belts). Experimental results show that the proposed methods effectively suppress noise and harmonic interference. At a distance of 1.5 m, the accuracy of breathing rate detection with an error of less than 3 bpm is 100%, while the accuracy for heart rate is 87%. At a distance of 3.0 m, the accuracy of breathing rate detection with an error of less than 3 bpm is 75%, and the accuracy for heart rate is 68.75%. These results validate the feasibility and effectiveness of FMCW radar in remote monitoring of vital signs in multiple subjects. Future research can focus on two aspects: improving the accuracy of long-range monitoring by tracking the breathing and heart rate of dynamic subjects, and further exploring the use of millimeter-wave radar technology to detect human blood pressure.

REFERENCES

[1] M. Zhou, Y. Liu, S. Wu, C. Wang, Z. Chen, and H. Li, "A novel scheme of high-precision heart rate detection with a mm-wave FMCW radar," IEEE Access,vol. 11, pp. 85118-85136, 2023.

[2] C. Li, Y. Bian, Z. Zhao, Y. Liu, and Y. Guo, "Advances in Biointegrated Wearable and Implantable Optoelectronic Devices for Cardiac Healthcare," (in eng), Cyborg Bionic Syst, vol. 5, p. 0172, 2024, doi: 10.34133/cbsystems.0172.

[3] Y. Zhao, V. Sark, M. Krstic, and E. Grass, "Multi-target vital signs remote monitoring using mmWave FMCW radar," in 2021 IEEE Microwave Theory and Techniques in Wireless Communications (MTTW), 2021: IEEE, pp. 290-295.

[4] J Lázaro et al., "Electrocardiogram Derived Respiratory Rate Using a Wearable Armband," in IEEE Transactions on Biomedical Engineering, vol. 68, no. 3, pp. 1056-1065, March 2021.

[5] X. Zhang, X. Yang, Y. Ding, Y. Wang, J. Zhou, and L. Zhang, "Contactless simultaneous breathing and heart rate detections in physical activity using ir-uwb radars," Sensors, vol. 21, no. 16, p. 5503, 2021.

[6] P. Kontou, S. B. Smida, S. N. Daskalakis, S. Nikolaou, M. Dragone, and D. E. Anagnostou, "Heartbeat and respiration detection using a low complexity cw radar system," in 2020 50th European Microwave Conference (EuMC), 2021: IEEE, pp. 929-932.

[7] S. Xue, Z. Xu, Y. Wang, J. Shi, and A. C. Yucel, "Simultaneous multi-person vital signs monitoring using multiple-input multiple-output FMCW millimeter wave radar," AEU-International Journal of Electronics and Communications, vol. 188, p. 155578, 2025.

[8] E.-K. Wu et al., "Non-contact monitoring of human cardiorespiratory activity during sleep using FMCW millimeter wave radar," Measurement, vol. 242, p. 116144, 2025.

[9] H. Wang et al., "HeRe: Heartbeat signal reconstruction for low-power millimeter-wave radar based on deep learning," IEEE Transactions on Instrumentation and Measurement, vol. 72, pp. 1-15, 2023.

[10] F. Wang, X. Zeng, C. Wu, B. Wang, and K. R. Liu, "Driver vital signs monitoring using millimeter wave radio," IEEE Internet of Things Journal, vol. 9, no. 13, pp. 11283-11298, 2021.

[11] F. Wang, X. Zeng, C. Wu, B. Wang, and K. R. Liu, "mmHRV: Contactless heart rate variability monitoring using millimeter-wave radio," IEEE Internet of Things Journal, vol. 8, no. 22, pp. 16623-16636, 2021.

[12] B. R. Upadhyay, A. B. Baral, and M. Torlak, "Vital sign detection via angular and range measurements with mmWave MIMO radars: Algorithms and trials," IEEE Access, vol. 10, pp. 106017-106032, 2022.

[13] M. Mercuri, I. R. Lorato, Y.-H. Liu, F. Wieringa, C. V. Hoof, and T. Torfs, "Vital-sign monitoring and spatial tracking of multiple people using a contactless radar-based sensor," Nature Electronics, vol. 2, no. 6, pp. 252-262, 2019/06/01 2019, doi: 10.1038/s41928-019-0258-6.

[14] Y. Xiong, Z. Peng, C. Gu, S. Li, D. Wang, and W. Zhang, "Differential enhancement method for robust and accurate heart rate monitoring via microwave vital sign sensing," IEEE Transactions on Instrumentation and Measurement, vol. 69, no. 9, pp. 7108-7118, 2020.

[15] W. Lv, W. He, X. Lin, and J. Miao, "Non-contact monitoring of human vital signs using FMCW millimeter wave radar in the 120 GHz band," Sensors, vol. 21, no. 8, p. 2732, 2021.

[16] Z. Ling, W. Zhou, Y. Ren, J. Wang, and L. Guo, "Non-contact heart rate monitoring based on millimeter wave radar," IEEE Access, vol. 10, pp. 74033-74044, 2022.

[17] M. Alizadeh, G. Shaker, J. C. M. D. Almeida, et al. Remote Monitoring of Human Vital Signs Using mm-Wave FMCW Radar[J]. IEEE Access, 2019, 7: 54958-54968.

[18] A. Lazaro, M. Lazaro, R. Villarino, and D. Girbau, "Seat-occupancy detection system and breathing rate monitoring based on a low-cost mm-wave radar at 60 ghz," IEEE Access, vol. 9, pp. 115403-115414, 2021.

[19] Z. Hao, Y. Wang, F. Li, G. Ding, and Y. Gao, "Mmwave-RM: A respiration monitoring and pattern classification system based on mmwave radar," Sensors (Basel, Switzerland), vol.24, no. 13, p. 4315, 2024.

[20] IWR6843 Single-Chip 60-GHz to 64-GHz Industrial Radar Sensor Evaluation Module. Available online:https://www.ti.com.cn/tool/cn/IWR6843ISK (accessed on 27 December 2024).

[21] DCA1000EVM Real-time Data-capture Adapter For Radar Sensing Evaluation Module. Available online:https://www.ti.com/tool/DCA1000EVM (accessed on 27 December 2024).

[22] Z. Xu et al., "Simultaneous monitoring of multiple people's vital sign leveraging a single phased-MIMO radar," IEEE Journal of Electromagnetics, RF and Microwaves in Medicine and Biology, vol. 6, no. 3, pp. 311-320, 2022.

[23] S. Ahmed, M. Abdullah, and M.-S. Alouini, "mm-Wave Radar-Based Multiple Patients' Breathing and Heart Rates Measurement," 2023.